Title

Unsteady Flow Simulation and Erosion Assessment in a Ditch Network of a Drained Peatland Forest Catchment in Eastern Finland

Journal

Water Resources Management, 28(14)

ISSN

0920-4741

Authors

Haahti, Kersti
Younis, Bassam A
Stenberg, Leena
et al.

Publication Date

2014-11-01

DOI

10.1007/s11269-014-0805-x

Peer reviewed

Water Resour Manage (2014) 28:5175–5197
DOI 10.1007/s11269-014-0805-x

Unsteady Flow Simulation and Erosion Assessment in a Ditch Network of a Drained Peatland Forest Catchment in Eastern Finland

Kersti Haahti · Bassam A. Younis · Leena Stenberg · Harri Koivusalo

Received: 17 June 2014 / Accepted: 29 September 2014 /
Published online: 7 October 2014

Abstract We developed and applied a computational model for simulating unsteady flow in a drainage network of a boreal forested peatland site. The input to the model was the hourly runoff produced by a hydrological model. The simulations of the flow in the ditch network were performed using an iterative procedure for solving the Saint-Venant equations that govern the flow in each of the network channels. These equations were solved separately for each ditch branch, and the flow depths at the junctions were corrected using the method of characteristics. The model was applied to the drainage network of a peatland catchment in Eastern Finland over a period of 15 months. Because flow resistance in the ditches depended strongly on flow conditions, flow resistance (Manning's n) was introduced as a function of discharge. The model was calibrated and validated against field data and the simulation results were further applied to assess erosion risk. The highest risk of erosion occurred during long lasting flows induced by snowmelt at ditch sections with a steep slope and a large upstream area. These model results can aid in the design and siting of water protection measures within the drained area.

Keywords Hydraulic modeling · Erosion risk · Drainage · Forestry · Manning's n · Peatland

1 Introduction

Peatland and wetland drainage has been an important component of forestry management practices in Northern Europe, the British Isles, Russia, and some areas of the United States and Canada covering a total land area of about 15 million ha (Paavilainen and Päivänen 1995). In Fennoscandinavia, peatlands have been drained extensively in the 1960s–1970s (Iritz et al. 1994; Joensuu et al. 1999). The largest forest drainage areas are in Finland where 4.7 million

K. Haahti (✉) · L. Stenberg · H. Koivusalo
Department of Civil and Environment Engineering, Aalto University School of Engineering,
FI-00076 Aalto, Finland
e-mail: kersti.haahti@aalto.fi

B. A. Younis
Department of Civil and Environmental Engineering, University of California, Davis, CA 95616, USA

ha of peatlands are drained, amounting to about half of the total land area of peatlands in the country (Finnish Forest Research Institute 2013). Nowadays artificial drainage is rarely conducted on pristine peatlands, and the focus in Finland has switched to the maintenance of existing ditch networks (Peltomaa 2007) while in the United Kingdom, for example, drain blocking is increasingly being applied to restore peatlands (Armstrong et al. 2009). It is estimated that one third of the drained peatlands in Finland are in need of ditch network maintenance in order to sustain forest productivity (Koivusalo et al. 2008a). The ditch network maintenance has adverse environmental impacts through channel erosion and transport of suspended solids (SS) into the receiving rivers and lakes (Joensuu et al. 1999; Prévost et al. 1999). According to Joensuu et al. (1999), the SS load increases markedly after ditch network maintenance operations and remains high especially during the first post-treatment year. The risk of erosion has also been reported to further increase when the ditches are cut into mineral soil (Carling et al. 1997; Joensuu 2002). Marttila and Kløve (2010) report that the majority of the SS load on drained peatland sites in Finland is generated during summer peak discharges and spring season snowmelt.

Among forestry activities in Finland, the SS load after ditch network maintenance on peatlands causes one of the largest strains on surface waters (Marttila et al. 2010). In earlier studies the excess loads by forestry activities have been determined in catchment scale using the paired catchment approach (e.g. Joensuu et al. 1999; Nieminen et al. 2010). Such an approach is useful for quantifying the load magnitudes, but does not provide information about the processes at the areas within the ditch network where the sources of erosion occur. Water protection methods, such as breaks in cleaning, silt traps, and peak runoff control structures (Marttila et al. 2010) as well as peatland restoration measures such as ditch blockage (Armstrong et al. 2009) have been introduced to reduce the loads from drained peatland sites. The design and siting of these measures call for the description and quantification of the hydraulic conditions within ditch networks that drive erosion and transport of SS. Holden et al. (2007) reported that the bottom slope and the upstream catchment area explained most of the erosion occurring in the ditches and suggested that the bottom slope could be used as a simple variable to aid decision-making on drain blocking. Lappalainen et al. (2010) proposed one of the few sediment transport models tailored for drained peatland environments. Their model simulates erosion, sedimentation, and SS transport in a single collector ditch. Tuukkanen et al. (2012) presented a study of erosion risk assessment within an entire forest ditch network that was based on a simple steady-state solution of a design discharge solved with the RiverLifeGIS decision support tool (Lauri and Virtanen 2002). The RiverLifeGIS software is based on the D8 method (Jenson and Domingue 1988) and Manning's equation which implies that flow cannot be divided at a diverging junction of the network and that the downstream flow conditions cannot affect the flow upstream. The present study was motivated by the need to develop a more sophisticated simulation tool that can be used for the assessment of erosion risk in forest ditch networks.

The simulation of unsteady flow in open channels typically rests on the numerical solution of the Saint-Venant equations. Compared to a single ditch, flow routing in a network is more complicated due to the presence of backwater effects at the junctions which necessitate the simultaneous solution for flow in all the connected channels (Islam et al. 2005). Efficient algorithms to solve unsteady flow in general channel networks (e.g. Sen and Garg 2002; Zhu et al. 2011) are most suitable for simulating flow in complex drainage networks. Obtaining accurate simulations of flows in channels rests on the accurate estimation of flow resistance. The most common method for quantifying resistance is Manning's equation, where coefficient n describes surface roughness and is well-documented for different surfaces. However, the values of Manning's n presented in the literature are usually obtained for mean or high flow

conditions, and for larger channels than typical drainage ditches (Hosia 1980). In large streams with fully turbulent flow, Manning's n is nearly constant but for transitional or laminar flow, its value is expected to vary with changing flow conditions (Cunge et al. 1980; Yen 2002). Additionally, in small streams with low flow conditions, the relative effect of the bed roughness and individual obstacles increases causing a higher flow resistance (Lee and Ferguson 2002; Järvelä and Helmiö 2004). The variation of flow resistance has previously been related to Reynolds number, discharge, flow velocity and flow depth (e.g. Hosia 1980; Abdelsalam et al. 1992; Järvelä and Helmiö 2004). Because of the empirical nature of Manning's n, model calibration is an essential step in the application of flow simulation models (Cunge et al. 1980).

The objectives of this study were to develop a computational model for unsteady flow in channel networks, and to apply the model to a maintained ditch network of a small peatland forestry catchment in Eastern Finland. The goal was to assess erosion risk based on the hydraulic conditions simulated by the developed model. Since the flow resistance in the small ditches was expected to vary with the flow conditions, the challenge in the computations was to relate Manning's n to discharge. The hydrological FEMMA model (Koivusalo et al. 2006) was applied to produce inflow to the open ditches from the forested land areas and the hydraulic model for the ditch network was run for 15 months after the maintenance of the ditches. The erosion risk in the drainage network was then assessed using the simulated flow velocity and bed shear stress (Graf 1984).

2 Material

2.1 Site Description

The study site was the Koivupuro catchment which is a 113 ha drained peatland area in Eastern Finland (63°53′ N, 28°40′ E; Fig. 1). During 1981–2010 the mean annual air temperature in the area was 2.3 °C and the mean annual precipitation 591 mm (Pirinen et al. 2012). The Koivupuro catchment was initially drained by an open ditch network in 1983 for forestry purposes and has been monitored since 1978. In August 2011, the majority of the Koivupuro catchment ditch network was maintained and a smaller nested catchment was set up in the area for intensive monitoring (Fig. 1). The ditches at the edges of the nested catchment were blocked.

The present study was focused on the small nested catchment in the Koivupuro area (Fig. 1). The nested catchment was 5.2 ha in size and the total length of the cleaned ditches was 1.6 km. The ditch spacing was approximately 35 m. The ditches left unmaintained in the nested catchment in August 2011 (approximately 0.1 km) were expected to have a minor role in conducting water out of the area.

The soil type of the experimental area was mostly peat (Fig. 1). The depth of the peat layer varied in the range 0–4 m. The peat was classified as either woody sphagnum peat (LS) or woody sphagnum-carex peat (LSC). The decomposition of peat in the area was characterized as 3–8 on the von Post scale (von Post 1922). The majority of the ditches in the nested catchment were peat down to the ditch bottom, with only a few reaching the mineral soil.

The study area was slightly sloping (with a mean slope of 1 %), the highest areas being in the northern part and the lowest in the southeastern part of the catchment. The area was covered by a Scots pine (*Pinus sylvestris*) dominated stand with a mixture of Norway spruce (*Picea abies*) and Birch (*Betula pendula*). The stand volume was 89 m^3 ha^{-1} in 2012.

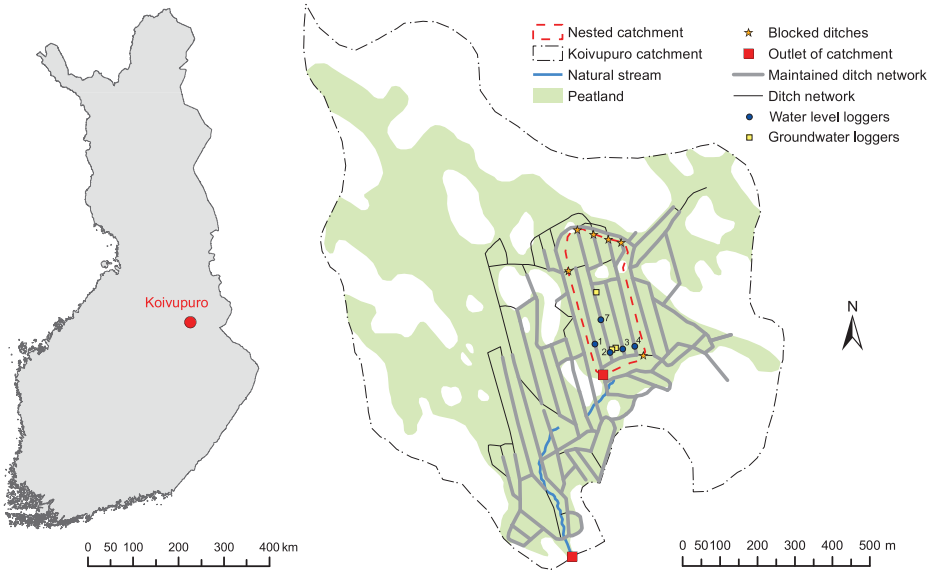

Fig. 1 Location of the Koivupuro catchment in Eastern Finland and the smaller nested catchment formed in the area after ditch network maintenance in August 2011

2.2 Measurements

Meteorological data were available from a weather station of the Finnish Forest Research Institute called Iso-Kauhea located 3 km from the Koivupuro catchment. The data included air temperature, precipitation, relative humidity, and global radiation recorded at a 20 min interval. Reference meteorological data from two nearby weather stations, Sotkamo (30 km) and Valtimo (26 km), of the Finnish Meteorological institute (FMI) were available to complete the data requirements.

The number of stems, the diameter at breast height (DBH) and the stand height were determined using systematically selected experimental plots inside the nested catchment. Each characteristic was determined separately for Scots pine, Norway spruce, and Birch.

The water level in the ditches was measured at 5 locations (Fig. 1) and the groundwater table at 3 locations using automatic Trutrack WT-HR Water Height loggers. Measurements were taken at a resolution of 1 mm every 15 min during the frost free period since August 2011. The loggers were placed in perforated pipes installed at the bottom of the ditch or in the ground. The stage of the bottom of the loggers was leveled in 2011 and 2013.

Discharge was measured at the outlets of both the nested catchment and the entire catchment (Fig. 1) using V-notch weirs and pressure sensors. Water stage was measured by the pressure sensors every 15 min during the frost free period. The accuracy of the stage measurement was checked by regular manual water depth measurements. At the outlet of the nested catchment, the discharge was produced using the stage-discharge relationship:

$$Q = 1.381(h - h_{weir})^{2.5} \quad (1)$$

where Q [m^3 s^{-1}] is the discharge, h [m] is the flow depth at the weir and h_{weir} [m] is the distance from the bottom of the ditch to the bottom of the V-notch (0.27 m).

In September 2011, the bottom elevation of all the cleaned ditches of the nested catchment was leveled every 10 m to an accuracy of 0.01 m. Furthermore, a 10×10 m^2 digital elevation model (National Land Survey of Finland) was available for the catchment area.

3 Methods

3.1 Modeling Inflow to Drainage Ditches

The runoff entering the open ditch network of the nested Koivupuro catchment was estimated by the forest hydrological model FEMMA, which has been earlier applied to study the hydrological impacts of forestry practices in boreal conditions (Koivusalo et al. 2006, 2008b). The model reads meteorological data as input and calculates the water balance components. The model simulates interception and transpiration of over- and understorey vegetation, soil and groundwater movement, and runoff generation at an hourly resolution. In winter, the model accounts for snow accumulation, snowmelt, and ground freezing.

The input meteorological data consisted of hourly time series of air temperature, precipitation, wind speed, relative humidity, global radiation and long-wave radiation. Apart from long-wave radiation, all the variables were measured at the Iso-Kauhea station. Occasional missing values in the Iso-Kauhea data, winter time precipitation, and wind speed were replaced with data from the FMI weather stations. Long-wave radiation was estimated based on the measurements of air temperature, relative humidity and global radiation (Allen et al. 2006; Turunen 2011). The canopy model included in FEMMA (Koivusalo et al. 2006) uses meteorological data above the forest canopy as input and simulates throughfall, net radiation, and wind speed beneath the forest canopy. The model simulates interception of rain or snowfall and unloading of intercepted snow in the overstorey vegetation layer. Throughfall can be intercepted by understorey vegetation, which can be covered with ground snow during freezing air temperatures. Interception evaporation and transpiration in the vegetation layers are simulated based on the Penman-Monteith type combination equation (e.g. Wigmosta et al. 1994). Ground snow processes are simulated by a coupled energy and mass balance snow model.

The parameters required to characterize vegetation are the mean stand height, the mean DBH, the leaf area index (LAI), and the canopy density for both under- and overstorey. The understorey canopy density was set to the value of 1 (i.e. 100 % coverage). Based on the stand measurements, the LAI and the canopy density of the stand were estimated to be 1.6 m^2 m^{-2} and 0.7 respectively (Haahti 2014).

The soil water movement and runoff generation is modeled by FEMMA in a typical longitudinal section (vertical 2D profile) from a water divide to an open channel. This profile is divided into vertical soil columns and into horizontal soil layers. The vertical distribution of the peat soil hydraulic properties was adopted from Smolander (2011). The vertical fluxes in the unsaturated zone of the soil columns are computed based on a numerical solution of Richard's equation. Water that cannot infiltrate is transported downslope as surface runoff until it either reaches the ditch or infiltrates into the soil. The lateral groundwater flow between the soil columns is computed according to Darcy's law. As a boundary condition the groundwater flow model needs the water level in the ditch. In FEMMA the groundwater flow toward the ditches is activated when the water level in the downslope soil column of the profile rises above the ditch water level. It should be noted that the model does not account for lateral groundwater flow beneath the ditch network, when the groundwater level is below the ditch bed. Furthermore, in FEMMA no groundwater flow is assumed to occur through the boundaries of the modeled area. The FEMMA model accounts for channel flow processes using a

simple delay function. A delay of 1 h was applied in the calibration of the hydrological model against the runoff measured at the outlet of the catchment. However, when the modeled runoff was used as the input to the hydraulic channel flow model, the delay was not applied.

The hydrological model was calibrated against measured discharge at the outlet of the nested catchment and the measured water table. This was achieved by adjusting the vertical and horizontal soil hydraulic conductivities, the coefficient α of the van Genuchten (1980) model of the water retention curve, and the global multiplication coefficient of potential evapotranspiration. The goodness of fit between the modeled and the measured runoff was evaluated using the Nash-Sutcliffe model efficiency coefficient, E_{NS} (Nash and Sutcliffe 1970). The calibration period was 8–27 July 2012, and the validation period was 1–20 June 2012. Finally the model was run from October 2011 until the end of 2012. During the winter period, the computed snow depth was evaluated against values obtained from the FMI weather stations and the coefficient for snowfall correction was adjusted.

The flow computed by the hydrological model was distributed to enter the ditch network according to the topography of the catchment. Based on the single-direction flow algorithm D8 (Jenson and Domingue 1988), the relative amount of flow entering from the upslope terrestrial areas to each computational node in the ditches was estimated.

3.2 Defining Network Characteristics

The channels and vertices in the network were numbered in no specific order (Fig. 2). The length of the branches varied from 16 to 278 m, and the average bottom slope was 0.0086. The connectivity of branches at junctions was stored in the form of an incidence matrix including the assumed flow directions (Kutija 1995).

The maintained ditches were cleaned using a digger whose shovel dimensions determined the shape of the channel cross section (Fig. 3). The sides of the cross section were approximated as arcs of a circle. Using this assumption, the spread (T [m]), the flow cross-sectional area (A [m^2]) and the wetted perimeter (P [m]) were determined as functions of flow depth (h):

$$T(h) = 2\left(\sqrt{r^2-(H-h)^2}-r+\frac{L_2}{2}\right) \tag{2}$$

$$A(h) = L_1 h + 2\int_a^b \sqrt{r^2-\delta^2}\,d\delta-(H-h)(T-L_1) \tag{3}$$

$$P(h) = L_1 + 2\int_a^b \frac{r}{\sqrt{r^2-\delta^2}}\,d\delta \tag{4}$$

where L_1 [m], L_2 [m], H [m] and r [m] are dimensions of the cross section (Fig. 3) and the integration interval is determined by a and b as follows:

$$a = -\sqrt{r^2-(H-h)^2} \tag{5}$$

and

$$b = \frac{L_2-L_1}{2}-r \tag{6}$$

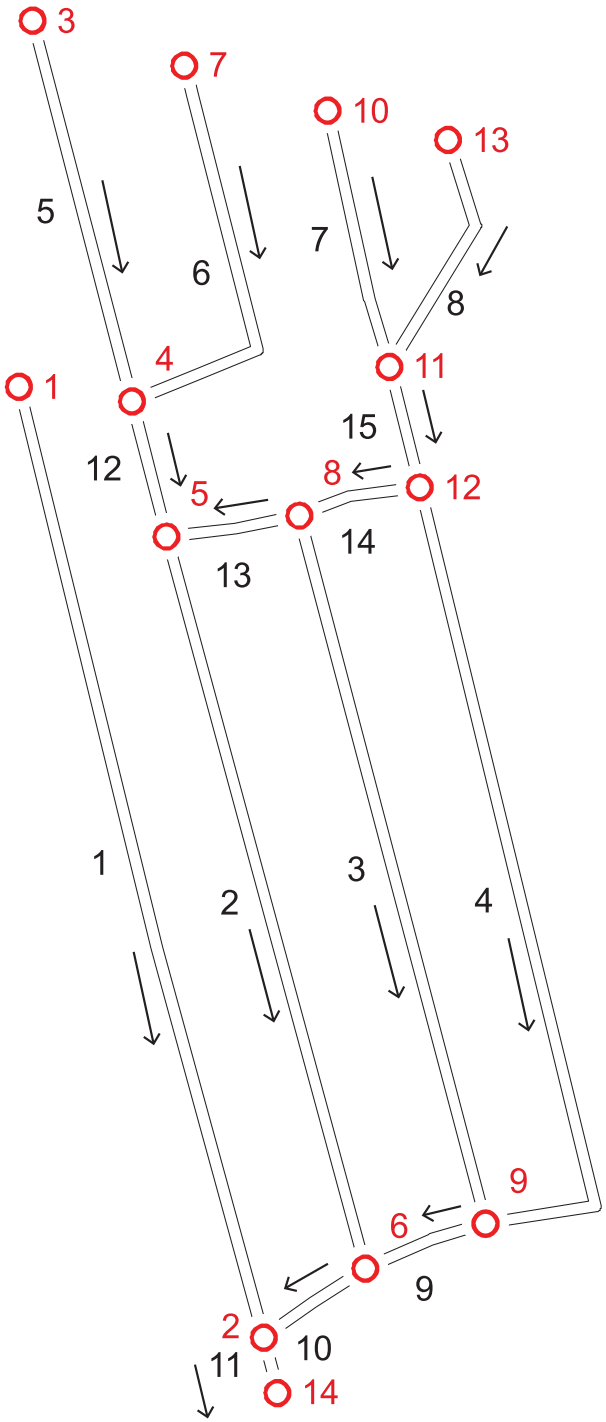

Fig. 2 Numbering of the channels and the vertices of the ditch network of the Koivupuro nested catchment with the assumed flow directions

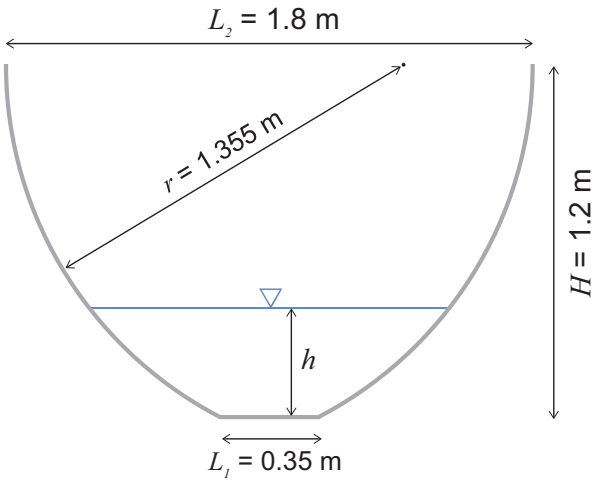

Fig. 3 Channel cross section of the maintained ditches in the Koivupuro catchment determined by the shovel used for ditch cleaning in August 2011

3.3 Flow Simulation in a Channel Network

The flow in the Koivupuro ditch network was simulated using the algorithm of Zhu et al. (2011). This algorithm was chosen for implementation into the model because it is applicable for both looped and dendritic channel networks, does not require a specific node numbering scheme, and it has been shown to accurately handle back-water effects. The developed model did not impose restrictions on the total number of branches, or on the number of branches connected to a single junction. The algorithm consists of an iterative procedure where the flow in each of the channels of the network is solved separately using the Saint-Venant equations, and the flow depth at the junctions are corrected at each iteration using the method of characteristics. This process is repeated until convergence is reached (Fig. 4).

3.3.1 Governing Equations and Their Discretization

The one-dimensional unsteady flow in open channels is governed by the Saint-Venant equations which can be written as:

$$\frac{\partial A}{\partial t} + \frac{\partial Q}{\partial x} - q = 0 \tag{7}$$

$$\frac{\partial Q}{\partial t} + \frac{\partial}{\partial x}\left(\frac{Q^2}{A}\right) + gA\frac{\partial h}{\partial x} + gA\left(S_f - S_0\right) = 0 \tag{8}$$

where A [m^2] is the cross-sectional flow area, Q [m^3 s^{-1}] is the discharge, q [m^2 s^{-1}] is the lateral inflow per unit length, h [m] is the flow depth, g [m s^{-2}] is the

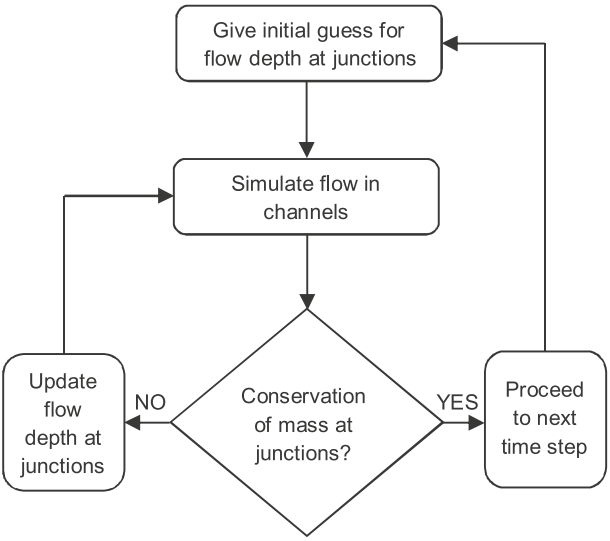

Fig. 4 Flowchart of the algorithm proposed by Zhu et al. (2011) to simulate flow in a general channel network

gravitational acceleration, S_f is the friction slope, S_0 is the bottom slope, x [m] is the longitudinal distance along the channel and t [s] is time. The friction slope is estimated from Manning's equation:

$$S_f = \frac{n^2 Q|Q|}{A^2 R^{4/3}} \tag{9}$$

where R [m] is the hydraulic radius and n is Manning's resistance coefficient. Because the flow in the Koivupuro drainage network was not fully turbulent and the ditches were small, the influence of bed roughness and small obstacles was amplified, and appropriate values of Manning's n could not be adopted directly from the literature (Lee and Ferguson 2002; Yen 2002). Consequently, and based on evaluation of the flow depth and discharge measurements at Koivupuro (Haahti 2014), Manning's n was introduced as a function of the local discharge:

$$n(Q) = c|Q|^{-d} \tag{10}$$

where c and d are calibration parameters. The maximum value of Manning's n was capped at 4, which occurred in situations when the flow rate was at its minimum.

In order to compute unsteady flow, an initial steady-state solution for the flow in the network is required. The steady-state equations are derived from the Saint-Venant equations by neglecting the time derivatives (Cunge et al. 1980). Using finite differences, the steady-state continuity and momentum equations can be expressed as:

$$\frac{Q_{i+1} - Q_i}{\Delta x} - q^* = 0 \tag{11}$$

$$\frac{1}{\Delta x}\left[\left(\frac{Q^2}{A}\right)_{i+1} - \left(\frac{Q^2}{A}\right)_i\right] + gA^*\frac{h_{i+1} - h_i}{\Delta x} + g\left(\frac{n^2 Q|Q|}{AR^{4/3}}\right)^* - gA^* S_{0,i+1/2} = 0 \tag{12}$$

where i refers to the i^{th} node in the channel and the star-values (*) are given by:

$$f^{*} = \frac{f_i + f_{i+1}}{2} \tag{13}$$

For unsteady flow, the variables are functions of both distance and time forming a computational grid (x, t). The widely used four-point Preissmann implicit scheme (e.g. Cunge et al. 1980) was chosen to discretize the full Saint-Venant equations. This yields:

$$\frac{\left(A_i^{k+1} + A_{i+1}^{k+1}\right) - \left(A_i^{k} + A_{i+1}^{k}\right)}{2\Delta t} + \frac{\omega\left(Q_{i+1}^{k+1} - Q_i^{k+1}\right) + (1-\omega)\left(Q_{i+1}^{k} - Q_i^{k}\right)}{\Delta x} - q^{**} = 0 \tag{14}$$

$$\frac{\left(Q_i^{k+1} + Q_{i+1}^{k+1}\right) - \left(Q_i^{k} + Q_{i+1}^{k}\right)}{2\Delta t} + \frac{1}{\Delta x}\left\{\omega\left[\left(\frac{Q^2}{A}\right)_{i+1}^{k+1} - \left(\frac{Q^2}{A}\right)_{i}^{k+1}\right] + (1-\omega)\left[\left(\frac{Q^2}{A}\right)_{i+1}^{k} - \left(\frac{Q^2}{A}\right)_{i}^{k}\right]\right\}$$
$$+ gA^{**}\frac{\omega\left(h_{i+1}^{k+1} - h_i^{k+1}\right) + (1-\omega)\left(h_{i+1}^{k} - h_i^{k}\right)}{\Delta x} + g\left(\frac{n^2 Q|Q|}{AR^{4/3}}\right)^{**} - gA^{**}S_{0,i+1/2} = 0 \tag{15}$$

where i refers to the i^{th} node in the channel, k refers to the index of the time step, the star-values (**) refer to (16) and ω is the time weighting coefficient which was set to 0.6.

$$f^{**} = \frac{1}{2}\omega\left(f_{i+1}^{k+1} + f_i^{k+1}\right) + \frac{1}{2}(1-\omega)\left(f_{i+1}^{k} + f_i^{k}\right) \tag{16}$$

3.3.2 Simulating Flow in Channels

During the iteration process the flow in each branch of the network was simulated independently using the discretized Saint-Venant equations described in section 3.3.1. In addition to the continuity and momentum equations written for each reach of the channel, two further equations are required in the form of boundary conditions at the first and the last nodes. Boundary conditions can be known flow depths, known discharges or alternatively, a known relation between flow depth and discharge (Cunge et al. 1980).

To solve the non-linear system of equations, the iterative Newton–Raphson method was applied. The system of $2N$ equations (N is the number of nodes along the channel) can be expressed in the following form:

$$\mathbf{F}(\mathbf{\Phi}) = 0 \tag{17}$$

where $\mathbf{\Phi}$ is an array containing the $2N$ unknown variables. The iterative solution starts with an initial guess for the unknown variable vector ($\mathbf{\Phi}_I$) which is corrected by an error vector ($\Delta\mathbf{\Phi}$) until convergence is reached:

$$\mathbf{\Phi}_{I+1} = \mathbf{\Phi}_I - \Delta\mathbf{\Phi} = \mathbf{\Phi}_I - \mathbf{W}_I^{-1}\,\mathbf{F}(\mathbf{\Phi}_I) \tag{18}$$

where I is the index of the iteration round and $\mathbf{W}_I$ is the Jacobian matrix corresponding to the variable vector $\mathbf{\Phi}_I$. The Jacobian matrix for $\mathbf{F}(\mathbf{\Phi})$ needs thus to be formed (19) and the error vector can then be calculated according to (20).

$$\mathbf{W} = \frac{\partial \mathbf{F}(\mathbf{\Phi})}{\partial \mathbf{\Phi}} \tag{19}$$

$$\mathbf{W}_I \Delta \mathbf{\Phi} = \mathbf{F}(\mathbf{\Phi}_I) \tag{20}$$

To form the Jacobian matrix ($\mathbf{W}$), the discretized continuity and momentum equations are differentiated with respect to the unknown variables. While each equation in $\mathbf{F}(\mathbf{\Phi})$ depends only on the variables of the current node i and the node $i+1$, the Jacobian matrix will contain elements only in the band along the main diagonal. Banded matrix solution methods were therefore applied to solve the linear system (20). Finally the solution vector was updated using (18) and the procedure is repeated until a certain tolerance for both $|\Delta Q/Q|$ and $|\Delta h/h|$ is reached. Whereas the flow simulation in each channel of the network was independent, parallel processing was applied in the solution programming.

3.3.3 Correction of Flow Depth at Junctions

In channel networks, discontinuities are formed by channel junctions and separate equations need to be applied there to link the channels to each other. The so called inner boundary conditions are derived from the conservation of mass and energy (Cunge et al. 1980):

$$\sum Q = \sum Q_{in} - \sum Q_{out} = 0 \tag{21}$$

$$h_{in} = h_{out} \tag{22}$$

where subscript *in* refers to the incoming flows and *out* to the outgoing flows. The junction water stage prediction and correction method proposed by Zhu et al. (2011) is based on the method of characteristics. In this method, the initially guessed flow depth at the junctions (h_b) is corrected using the equation:

$$h_{bK+1} = h_{bK} + \Delta h_b \tag{23}$$

where K is the iterations index and Δh_b is the flow depth increment at the junctions. The latter is obtained from the characteristic curves derived from the Saint-Venant equations (Zhu et al. 2011):

$$\Delta h_b = \frac{\sum Q_{in} - \sum Q_{out}}{\sum \left(\sqrt{g A_{in} T_{in}} - \frac{Q_{in} T_{in}}{A_{in}} \right) + \sum \left(\sqrt{g A_{out} T_{out}} + \frac{Q_{out} T_{out}}{A_{out}} \right)} \tag{24}$$

Equations (23–24) are solved repeatedly until the value of $|\Delta h_b/h_b|$ drops below a pre-set tolerance.

3.3.4 Model Application and Evaluation

In the model applications to the ditch network of the nested catchment of Koivupuro, the flow at the upstream boundaries was set to zero and the downstream boundary at the catchment outlet was set according to Eq. (1). All the flow entering the channels was assumed to be through lateral inflow (which was produced by the hydrological FEMMA model) that was distributed along the ditches based on the topography (D8 method). To avoid dry-bed conditions, a lower limit of 0.5 l s^{-1} was set for the sum of lateral inflow.

A grid resolution of Δx=1 m and Δt=3,600 s was chosen for the simulations. The Preissmann four-point implicit scheme applied in the algorithm has been reported to be stable for any Courant number, meaning there are no requirements for the relationship of Δx and Δt (Szymkiewicz 2010). The distance step was set relatively short to avoid sawtooth profiles which are likely to arise during small flow depths (Strelkoff and Falvey 1993; Haahti 2014). A tolerance of 0.001 for $|\Delta Q/Q|$, $|\Delta h/h|$ and $|\Delta h_b/h_b|$ was set for all the simulations. To initiate the iterative procedure, constant flow depth and discharge in the whole channel network were specified.

The hydraulic model was calibrated against measured flow depth readings at the 5 locations in the network (Fig. 1) during 8–27 July 2012. For calibration, the sum of squared errors (*SSE*) between the measured and modeled flow depths was minimized by adjusting the two parameters, c and d, in Eq. (10). The minimization of *SSE* was performed using the built-in MATLAB optimization function which uses the Nelder-Mead simplex algorithm as described in Lagarias et al. (1998). The hydraulic model performance was evaluated using E_{NS} during the same calibration and validation periods as the hydrological FEMMA model (section 3.1).

3.4 Evaluation of Potential Erosion

The erosion risk in the ditch network was assessed over space and time by evaluating flow velocity v [m s^{-1}] and bed shear stress τ_b [N m^{-2}]. Bed shear stress was calculated at each node over the whole simulation period using the equation for reach-average bed shear stress (e.g. Biron et al. 2004):

$$\tau_b = \rho g R S_f \tag{25}$$

where ρ is the density of water [kg m^{-3}] and S_f is estimated following Manning's Eq. (9). Manning's n, which here characterizes only the roughness associated with the bed material, was set equal to 0.03, as suggested by previous studies on drained peatland sites (Marttila and Kløve 2008; Lappalainen et al. 2010; Tuukkanen et al. 2012). The magnitudes of flow velocity and bed shear stress were evaluated against the critical values in terms of particle detachment reported for deposited peat sediments.

4 Results

4.1 Hydrological Processes

Calibration of the hydrological FEMMA model for the period 8–27 July 2012 led to a Nash-Sutcliffe coefficient between the measured and modeled discharge of 0.69. The validation period (1–20 July 2012) showed a comparable model performance with E_{NS}=0.79. The values of the calibrated model parameters are presented in Table 1. The saturated hydraulic

Table 1 Parameters of the calibrated hydrological FEMMA model applied to the forested land areas between the drainage ditches in the Koivupuro nested catchment

Soil depth range (m)	Porosity	Residual water content	Van Genuchten parameter α	Van Genuchten parameter β	Vertical hydraulic conductivity (cm h^{-1})	Horizontal hydraulic conductivity (cm h^{-1})
0–0.1	0.95	0.1	0.3[a]	1.4	20[a]	200[a]
0.1–0.2	0.92	0.09	0.03[a]	1.39	10[a]	100[a]
0.2–0.6	0.89	0.1	0.013	1.48	0.1…0.001	50…0.5
> 0.6	0.91	0.17	0.017	1.56	0.001	0.05…0.001
Global multiplication coefficient of potential evapotranspiration						1.2[a]
Correction coefficient for snowfall						1.3[b]

[a] Calibrated against runoff data

[b] Calibrated against snow depth data

conductivity of peat decreased strongly with depth in Koivupuro. The high conductivity values near the soil surface were the key calibration parameters controlling the simulated water table depth. Studies from Finnish peatland sites have observed conductivities of 10^{-4}–3×10^{-3} m s^{-1} (i.e. 36–1,080 cm h^{-1}) for surface peat and 10^{-8}–10^{-4} m s^{-1} (i.e. 0.0036–36 cm h^{-1}) for deeper soil depths (Päivänen 1973; Kløve 2000; Ronkanen and Kløve 2005). Simulation results for the whole modeling period, October 2011–December 2012, represented well the runoff generation (E_{NS}= 0.76) and the accumulation of snow (E_{NS}=0.86) in the nested catchment (Fig. 5). The model tended to underestimate high flow peaks and overestimate low flow peaks, which was affected by the quality of the precipitation data. The hourly resolution of the input precipitation data does not represent well an intensive precipitation event that lasts for a shorter period than 1 h. The underprediction of long term low flows may be an indication of groundwater discharge in the area which is not described by the model. Since the catchment was artificially delineated with ditches it is also possible that there is a subsurface hydrological connection between the surrounding areas and the study catchment (e.g. Koivusalo et al. 2008b). Due to measurement inaccuracy at the weir of the nested catchment, the discharge at the outlet weir of the whole Koivupuro catchment (113 ha, Fig. 1) was used before 1 June 2012 for assessment of model performance. At the outlet of the larger catchment the runoff dynamics are expected to be more attenuated but the correlation between the hourly runoff series of two catchments (0.83) suggested that the large catchment data could be used to check the timing of the peak flows.

The computed results for flow accumulation into the ditches at a 1 m interval are illustrated in Fig. 6. The spatial distribution of runoff entrance to the ditch network was highly variable. For example, 3.2 % (50 nodes) of the network received no runoff at all, while 3.0 % (47 nodes) received one half of the total runoff entering the network. The flow accumulation scheme is affected by the D8 method which provides no possibility for flow divergence into two directions or to a direction somewhere between the eight possible directions.

4.2 Hydraulics in the Ditch Network

Figure 7 shows the simulated flow depth for the calibration period (8–27 July 2012) at the 5 flow depth measurement loggers. The measured flow depths are presented as bands which are

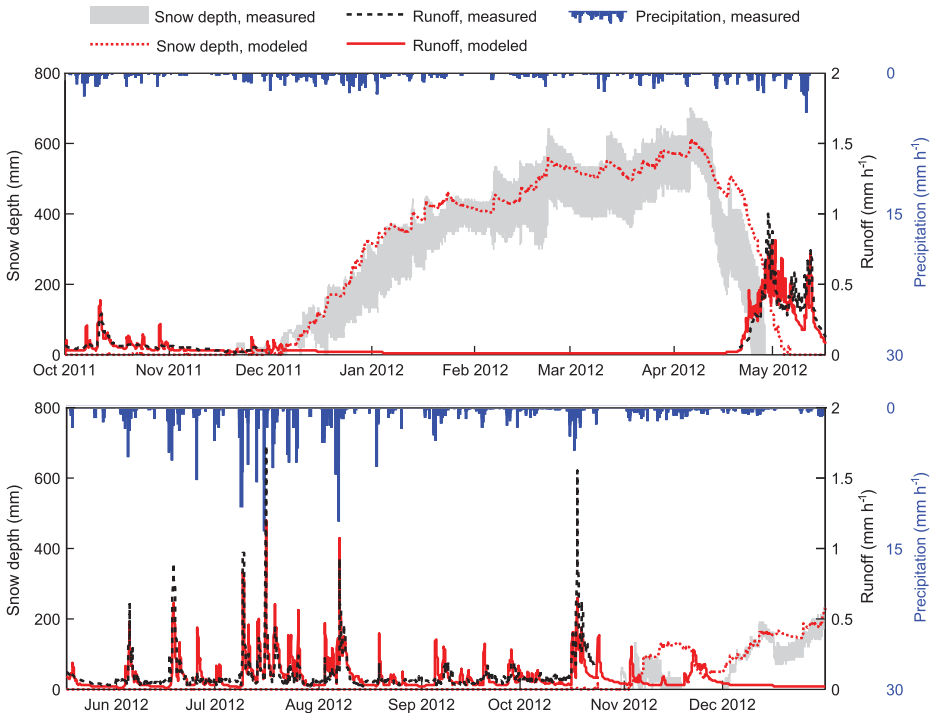

Fig. 5 Runoff and snow depth modeled by the hydrological FEMMA model compared to measured precipitation, runoff and snow depth (range limited by snow depth measurements at the two FMI weather stations) at the Koivupuro nested catchment during the simulation period October 2011–December 2012

limited by the ditch bottom leveling measurements in 2011 and 2013. Minimizing *SSE* between measured and modeled flow depth for the calibration period led to the following relationship between Manning's n and the local discharge:

$$n = 0.0074Q^{-0.66} \tag{26}$$

According to (26), Manning's n increases rapidly when the local discharge falls below 2 l s^{-1}. During the simulation period, Manning's n varied in the range 0.12–4. It is noteworthy that the high values of n in these small ditches characterize not only the bed material roughness but also other energy losses such as those due to leaf and needle litter at the bottom of the ditches (Fig. 8). The overall Nash-Sutcliffe coefficient between modeled and measured flow depths for the calibration period was E_{NS}=0.69 (Fig. 7). A similar good fit, E_{NS}=0.78, was observed between modeled and measured flow depths during the validation period (1–20 June 2012).

Simulation of the entire modeling period, October 2011–December 2012, revealed that there were periodic shifts in flow depth measurements (Fig. 9). At three out of five of the water stage loggers, the measured flow depths exhibited an obvious positive trend. During the leveling measurements in 2011 and 2013, changes in the ditch bottom levels were observed too. The measured bottom elevation at three loggers (1–3) rose between the leveling measurements. Furthermore, at logger 3, the suddenly increasing flow depth after mid-August 2012 is likely to be due to a damming effect caused by debris in the open ditch.

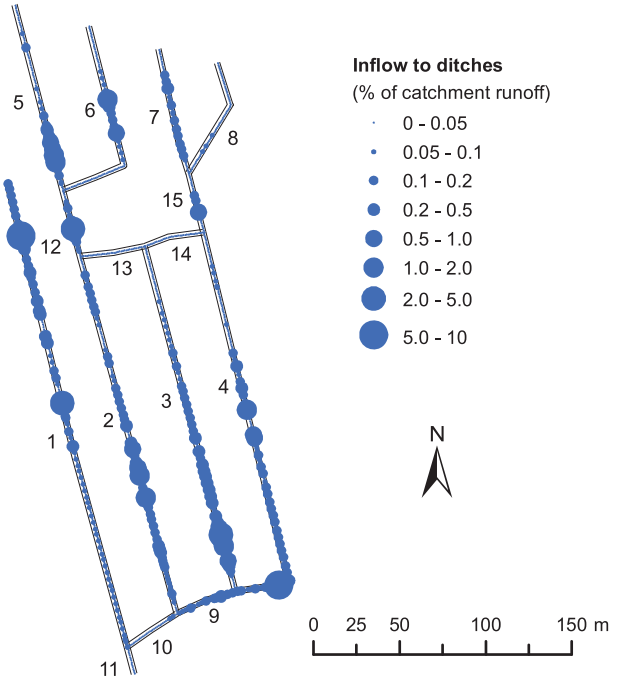

Fig. 6 Inflow to the open ditches at the Koivupuro nested catchment calculated using the D8 single flow direction algorithm

4.3 Erosion Risk Assessment

According to the model simulations, during the highest flow event, which occurred on 16 July 2012, the flow velocity in the ditch network of the Koivupuro nested catchment reached values up to 0.1 m s^{-1} and bed shear stress values up to 0.22 N m^{-2} (Fig. 10). Overall, values of velocity and bed shear stress were relatively low in the network ditches. Thus 82.0 % of the velocities remained below 0.04 m s^{-1} and 55.8 % of the bed shear stress values remained below 0.01 N m^{-2} during the time of the highest flow (Fig. 10). During the whole simulation period (Fig. 9), the respective values were 99.8 and 98.4 %. The spatial distributions of both flow velocity and bed shear stress (Fig. 10) suggest that the erosion risk was the highest in ditches 1 and 2, and in the collector ditches of the catchment (9–11). The location of the highest risk for erosion was in the steep southern end of ditch 2 where most of the flow accumulated. In the upstream feeder ditches (5–8), the discharge remained low even during this highest flow event on 16 July 2012.

The temporal velocity distribution at the southern end of the ditch 2 reveal that although velocities during intensive rainfall events reached higher values, the average flow velocity generated by spring snowmelt remained higher for an extended period of time (Fig. 11a–b). The same phenomenon was observed in the distributions of bed shear stress during snowmelt and the period of rainfall events (Fig. 11c–d). The tails of both shear stress distributions were however even longer than in the flow velocity distributions. The critical flow velocity for the surface layer of peat has been reported to be in the range 0.04–0.15 m s^{-1} (Kløve 1998; Marttila and Kløve 2008). Figure 11a–b show that during 55 % of the time in the spring snowmelt period, the flow velocity remained higher than the reported critical values while the

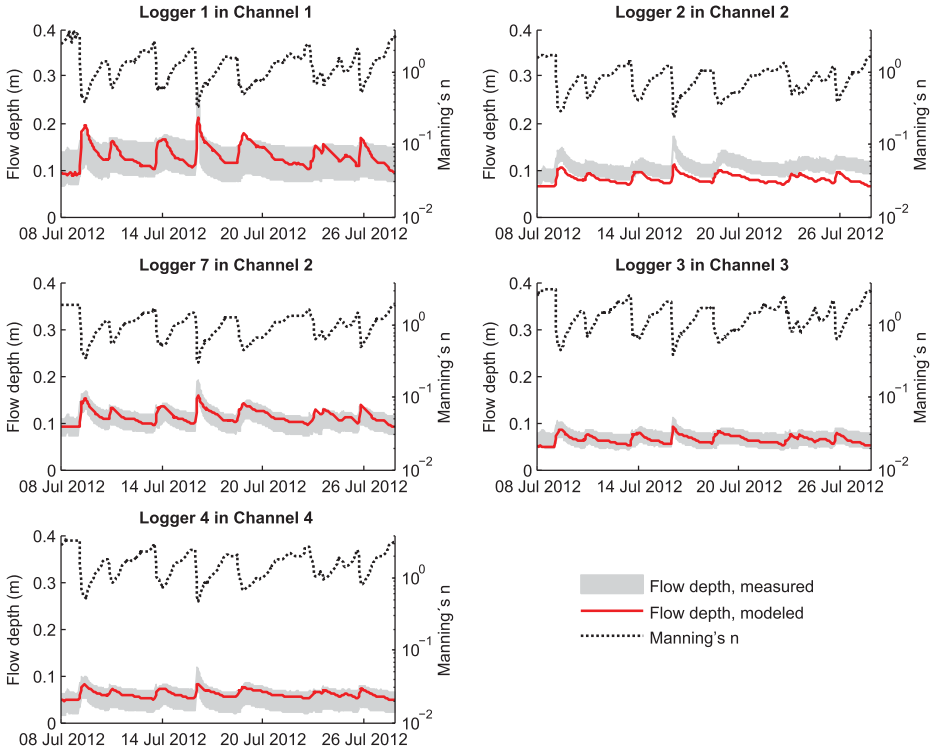

Fig. 7 Measured and modeled flow depth and the variation of Manning's *n* at 5 locations in the ditch network during the calibration period, 8–27 July 2012

corresponding probability for the period of summer rainfall events was only 16 %. For the case of bed shear stress, Marttila and Kløve (2008) observed two critical shear stress values for deposited peat sediments in laboratory flume experiments. They reported a lower critical shear stress of 0.01 N m^{-2} for the loose surface layer of peat, and a higher critical shear stress of 0.059 N m^{-2} for the entire peat bed. For the snowmelt period and the period of summer rainfalls, the lower critical limit was exceeded 92 and 50 % of the time, respectively (Fig. 11c–d). The critical shear stress for the whole peat layer (0.059 N m^{-2}) was exceeded during snowmelt with a probability of 26 % as the equivalent value for rainfall events was only 6 %.

5 Discussion

This study demonstrates a chain of computations to link local meteorological conditions to the ditch network flow regime and further to an assessment of erosion risk in a drained forested peatland catchment. Several prior studies have applied coupled hydrological and open channel flow models on drained agricultural and forested watersheds (Konyha and Skaggs 1992; Amatya et al. 1997; Giraud et al. 1997). The main difference between our application and those of previous studies is that we are more focused on the accurate representation of the hydraulics in the open channel network. Furthermore, our drainage network is much denser (spacing 35 m vs. 100–200 m) and we do not exclude the feeder ditches with low discharge

Fig. 8 Photograph of a ditch at Koivupuro during low flow conditions when Manning's *n* is high because of bed unevenness and obstacles causing separation of flow, and small riffle-pool sequences

from the flow routing model. Here the developed flow routing model for channel networks and its calibration against field measurements brought insight to the hydraulic conditions in small forest ditches. Flow resistance was found to be strongly dependent on discharge, allowing flow velocities to increase markedly only during high runoff events in the downstream parts of the network. It is well known that the erosive power of flowing water is the highest on steep reaches which gather large flow volumes (e.g. Holden et al. 2007; Lappalainen et al. 2010). While it is easy to identify the steep reaches in complex drainage networks, finding out the flow paths through a complex network requires the kind of modeling presented in this paper. The applied modeling approach can potentially be used to support planning of best practice ditch network maintenance (Joensuu et al. 2008) and to aid decision-making on drain blocking in peatland restoration projects (Armstrong et al. 2009).

Application of the developed model demonstrated the need for calibrating a hydraulic model against flow depth measurements in the actual catchment area. This is especially true for sites with dense drainage networks where low flow conditions occur. The practice of adopting Manning's *n* from the literature would lead to a considerable overestimation of flow velocities. Previous studies on Finnish drained peatland sites have utilized values of Manning's *n* in the range of 0.02–0.04 (Hosia 1980; Marttila and Kløve 2008; Lappalainen et al. 2010; Tuukkanen et al. 2012). Higher Manning's *n* in the Koivupuro ditches (n=0.12–4) are justifiable considering that low flow conditions tend to increase the effects of roughness elements in the ditches (Fig. 8; Lee and Ferguson 2002; Järvelä and Helmiö 2004). The continuously measured flow depth profiles also brought up the need for a resistance coefficient that varied according to the discharge. While the increase of flow resistance of up to 10-fold

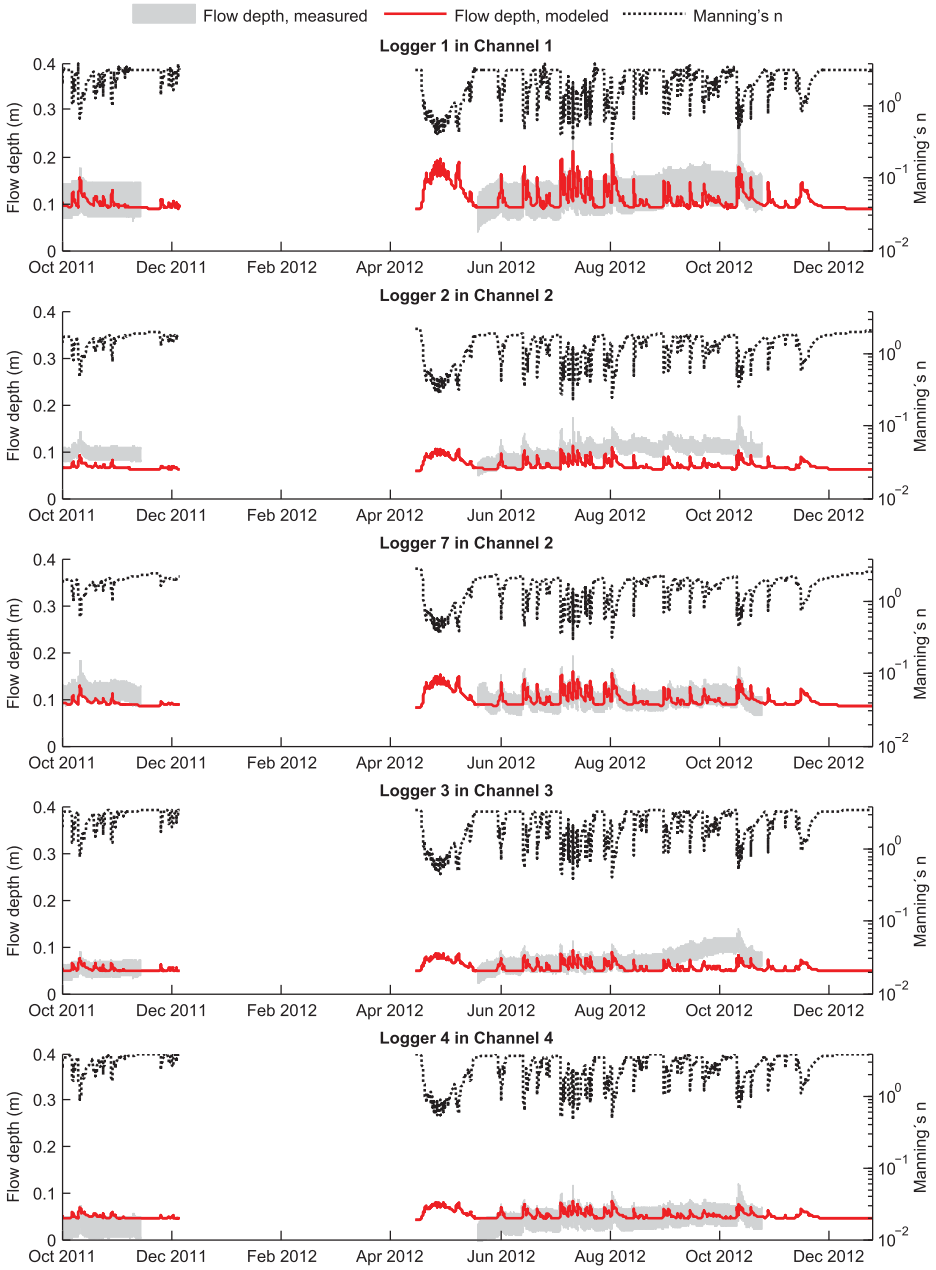

Fig. 9 Measured and modeled flow depth and the variation of Manning's *n* at 5 locations in the ditch network during the whole simulation period, October 2011–December 2012

with decreasing flow has been reported in field studies (e.g. Hosia 1980; Lee and Ferguson 2002), a resistance coefficient depending on flow conditions is seldom implemented in the simulation of unsteady flow in open channels. However in the case of flow through vegetation, Manning's Eq. (9) is typically modified e.g. by adjusting the exponents in (9) based on

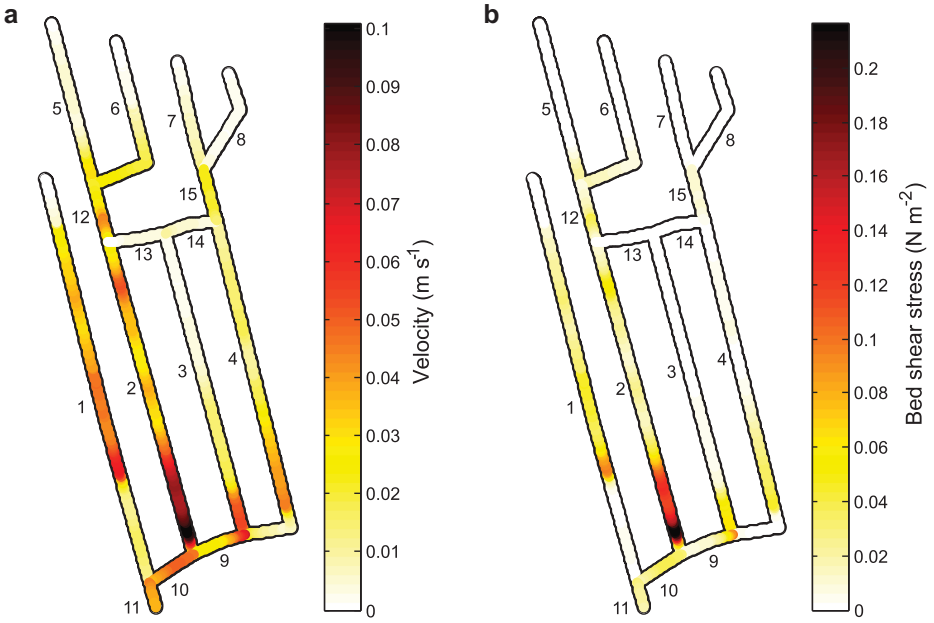

Fig. 10 Spatial distribution of flow velocity (**a**) and bed shear stress (**b**) in the ditch network during the highest flow peak on 16 July 2012

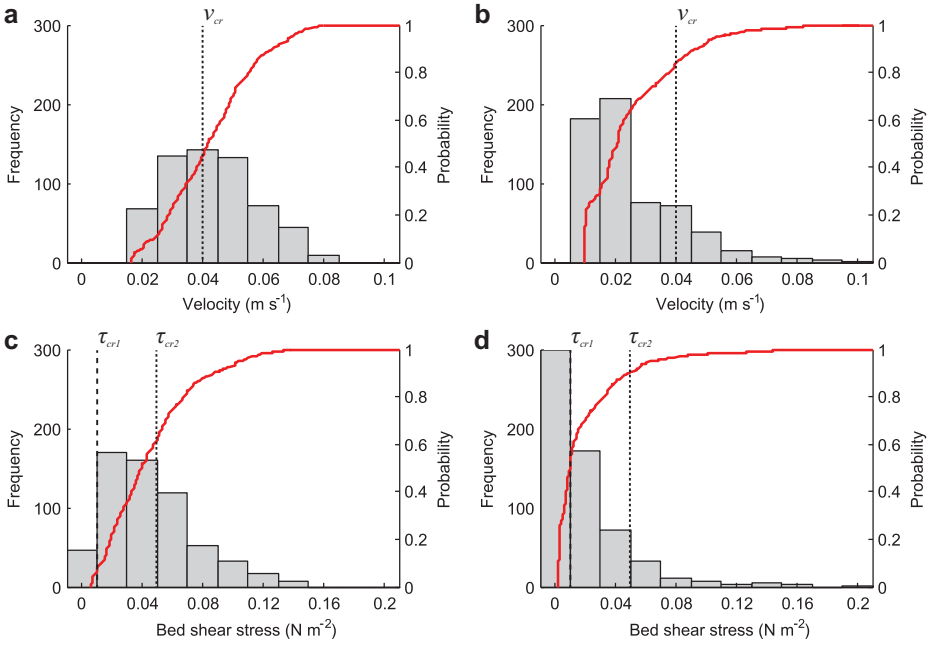

Fig. 11 Frequency and cumulative probability distribution functions for flow velocity and bed shear stress at the most critical point of the ditch network during spring season snowmelt (22 April–17 May 2012; **a** and **c**) and summer time rainfalls (6–31 July 2012; **b** and **d**). v_{cr}, τ_{cr1} and τ_{cr2} are critical values reported in the literature for peat (Kløve 1998; Marttila and Kløve 2008)

measurements during different flow conditions (Abdelsalam et al. 1992), which is comparable to the approach in this study where Manning's n is prescribed as a function of discharge. It should be noted that the resistance in Eq. (10) could be expressed as a function of flow depth instead of discharge. However, in Koivupuro discharge was found to yield better calibration results probably because discharge represented better the turbulence of the flow, which has also previously been related to an increase in resistance (e.g. Hosia 1980).

Tuukkanen et al. (2012) used a constant Manning's n of 0.022 for the entire ditch network in their steady-state flow computation, while their discharge ranged spatially in the range 0–0.08 $m^3 s^{-1}$. They applied the flow model to assess erosion risk and assumed that the erosion risk depended on flow velocity and the size of the upstream catchment area, which is directly related to the flow volume. This assumption implied that the critical flow velocity of the bed material was higher in the upstream areas of the ditch network where the discharge was low. However, the critical flow velocity is expected to be a property of the bed material, and thus should not depend on the flow (Graf 1984). The need for making such an assumption is explained by our finding that Manning's n should be higher in the feeder ditches where the discharge is lower.

In this study, the spatial assessment of flow velocity and bed shear stress highlighted the potentially most critical parts of the network in terms of erosion. The low flow velocity and bed shear stress evaluation suggested that deposition of sediments on the ditch bed would be likely. According to Stenberg et al. (2015) the sediments transported in the ditches are likely to originate from bank erosion processes driven by groundwater seepage or gravitation, especially in the case of mineral soil banks. Based on our results, scouring of the ditch bed can be expected only during the highest flow events in the parts of the Koivupuro ditch network where most of the flow accumulates and where the reaches are steep. When the ditch bed receives sediments from the eroding banks, detachment of these bed particles can be expected to occur readily during increased flow (Marttila and Kløve 2008). Also mineral bed load generated from upstream ditches that reach the mineral soil may affect the readiness of peat bed erosion downstream (Carling et al. 1997). In the nested catchment of Koivupuro the ditches are dug mostly in thick peat but outside the nested catchment several ditches are cut into mineral soil. Compared to the study of Tuukkanen et al. (2012), the present computational model extended the erosion risk estimate and demonstrated how the temporal distribution of flow velocity and bed shear stress reveal the different erosive power of spring snowmelt compared to the summer storms. According to the results, the major difference contributing to high SS loads during spring season snowmelt are due to the lasting high flow velocities rather than individual exceptionally high values.

6 Conclusions

A computational model for simulating unsteady flow in drainage networks was developed. Input to this model was provided by the FEMMA hydrological model that represented the water balance in the forested land areas between the drainage ditches and produced runoff input to the modeled ditch network. The flow model meets the needs of flow simulation in a drainage network on a forested peatland site and provides a basis for estimating spatial and temporal distribution of the risk of erosion within the network. An iterative algorithm for solving the Saint-Venant equations in a network of arbitrary number of channels and junctions was implemented. The model was tailored for small forest drainage ditches by prescribing the resistance coefficient as a function of discharge. Linking the hydraulic model with a hydrological model enabled the representation of the seasonal variability of flow conditions which

are driven by the meteorological data. The model can serve as a useful tool for assessment of spatial erosion risk within the ditch network, and assessment of temporal variation in erosion sensitivity. While this study is focused on the peatland forestry practices in Finland, peatland drainage is also performed in other boreal regions such as Russia and the United Kingdom (Paavilainen and Päivänen 1995). For maintenance practices heavily conducted on Finnish drained peatlands, the model provides insight to the design and allocation of water protection measures, such as silt traps and peak runoff control structures. The findings made in this study and the modeling approach may however also provide useful information to other practices on peatlands such as ditch blocking based restoration projects.

Acknowledgments The data were provided from the concentrated field measurements by the Finnish Forest Research Institute, University of Oulu, and Aalto University School of Engineering. We thank Hannu Marttila and Bjørn Kløve from the University of Oulu for their valuable comments on the manuscript. The Finnish Meteorological Institute is acknowledged for the meteorological data. Development of the computational model was performed while K. Haahti was a visiting scholar at the University of California, Davis. Funding for the study was kindly provided by the Aalto University School of Engineering and Maa- ja vesitekniikan tuki ry.

References

Abdelsalam M, Khattab A, Khalifa A, Bakry M (1992) Flow capacity through wide and submerged vegetal channels. J Irrig Drain Eng 118(5):724–732

Allen RG, Trezza R, Tasumi M (2006) Analytical integrated functions for daily solar radiation on slopes. Agric For Meteorol 139(1):55–73

Amatya D, Skaggs R, Gregory J (1997) Evaluation of a watershed scale forest hydrologic model. Agric Water Manag 32(3):239–258

Armstrong A, Holden J, Kay P, Foulger M, Gledhill S, McDonald A, Walker A (2009) Drain-blocking techniques on blanket peat: a framework for best practice. J Environ Manag 90(11): 3512–3519

Biron PM, Robson C, Lapointe MF, Gaskin SJ (2004) Comparing different methods of bed shear stress estimates in simple and complex flow fields. Earth Surf Process Landf 29(11):1403–1415

Carling PA, Glaister MS, Flintham TP (1997) The erodibility of upland soils and the design of preafforestation drainage networks in the United Kingdom. Hydrol Process 11(15):1963–1980

Cunge J, Holly F, Verwey A (1980) Practical aspects of computational river hydraulics. Pitman Advanced Pub. Program, Boston

Finnish Forest Research Institute (2013) Finnish Statistical Yearbook of Forestry

Giraud F, Faure J, Zimmer D, Lefeuvre J, Skaggs R (1997) Hydrologic modeling of a complex wetland. J Irrig Drain Eng 123(5):344–353

Graf WH (1984) Hydraulics of sediment transport. Water Resources Publication, Colorado

Haahti K (2014) Flow simulation in a ditch network of a drained peatland forest catchment in Eastern Finland. Master's Thesis, Aalto University, School of engineering, Department of Civil and Environmental Engineering

Holden J, Gascoign M, Bosanko NR (2007) Erosion and natural revegetation associated with surface land drains in upland peatlands. Earth Surf Process Landf 32(10):1547–1557

Hosia L (1980) Pienten uomien virtausvastuskerroin. Vesihallituksen tiedotus 199. Vesihallitus, Helsinki

Iritz L, Johansson B, Lundin L (1994) Impacts of forest drainage on floods. Hydrol Sci J 39(6):637–661

Islam A, Raghuwanshi N, Singh R, Sen D (2005) Comparison of gradually varied flow computation algorithms for open-channel network. J Irrig Drain Eng 131(5):457–465

Järvelä J, Helmiö T (2004) Hydraulic considerations in restoring boreal streams. Nordic Hydrol 35(3):223–235

Jenson S, Domingue J (1988) Extracting topographic structure from digital elevation data for geographic information system analysis. Photogramm Eng Remote Sens 54(11):1593–1600

Joensuu S (2002) Effects of ditch network maintenance and sedimentation ponds on export loads of suspended solids and nutrients from peatland forests. Dissertation, Finnish Forest Research Institute, Vantaa Research Centre

Joensuu S, Ahti E, Vuollekoski M (1999) The effects of peatland forest ditch maintenance on suspended solids in runoff. Boreal Environ Res 4(4):343–356

Joensuu S, Makkonen T, Vuollekoski M, Nieminen M, Leinonen A, Sarkkola S (2008) Metsätalouden vesiensuojelu. Vesitalous 6(2008):19–25
Kløve B (1998) Erosion and sediment delivery from peat mines. Soil Tillage Res 45(1):199–216
Kløve B (2000) Effect of peat harvesting on peat hydraulic properties and runoff generation. Mires and Peat 51(3):121–129
Koivusalo H, Kokkonen T, Laurén A, Ahtiainen M, Karvonen T, Mannerkoski H, Penttinen S, Seuna P, Starr M, Finér L (2006) Parameterisation and application of a hillslope hydrological model to assess impacts of a forest clear-cutting on runoff generation. Environ Model Softw 21(9):1324–1339
Koivusalo H, Hökkä H, Lauren A, Nikinmaa E, Laine J, Ahti E (2008a) Splitting the water balance of drained peatland forests into hydrological components. In: Farrell C, Feehan J (eds) After Wise Use – The Future of Peatlands: Proceedings of the 13th International Peat Congress. International Peat Society, Ireland, pp 485–487
Koivusalo H, Ahti E, Laurén A, Kokkonen T, Karvonen T, Nevalainen R, Finér L (2008b) Impacts of ditch cleaning on hydrological processes in a drained peatland forest. Hydrol Earth Syst Sci 12(5):1211–1227
Konyha K, Skaggs R (1992) A coupled, field hydrology: open channel flow model: theory. Trans ASAE 35(5): 1431–1440
Kutija V (1995) A generalized method for the solution of flows in networks. J Hydraul Res 33(4):535–554
Lagarias JC, Reeds JA, Wright MH, Wright PE (1998) Convergence properties of the Nelder-Mead simplex method in low dimensions. SIAM J Optimiz 9(1):112–147
Lappalainen M, Koivusalo H, Karvonen T, Lauren A (2010) Sediment transport from a peatland forest after ditch network maintenance: a modelling approach. Boreal Environ Res 15(6):595–612
Lauri H, Virtanen M (2002) A decision support system for management of boreal river catchments. Arch Hydrobiol 13(3–4):401–408
Lee AJ, Ferguson RI (2002) Velocity and flow resistance in step-pool streams. Geomorphology 46(1):59–71
Marttila H, Kløve B (2008) Erosion and delivery of deposited peat sediment. Water Resour Res 44(6):W06406
Marttila H, Kløve B (2010) Dynamics of erosion and suspended sediment transport from drained peatland forestry. J Hydrol 388(3–4):414–425
Marttila H, Vuori K, Hökkä H, Jämsen J, Kløve B (2010) Framework for designing and applying peak runoff control structures for peatland forestry conditions. For Ecol Manag 260(8):1262–1273
Nash J, Sutcliffe J (1970) River flow forecasting through conceptual models part I - a discussion of principles. J Hydrol 10(3):282–290
Nieminen M, Ahti E, Koivusalo H, Mattsson T, Sarkkola S, Laurén A (2010) Export of suspended solids and dissolved elements from peatland areas after ditch network maintenance in South-Central Finland. Silva Fenn 44(1):39–49
Paavilainen E, Päivänen J (1995) Peatland forestry: ecology and principles. Springer, Berlin
Päivänen J (1973) Hydraulic conductivity and water retention in peat soils. Acta For Fenn 129:1–70
Peltomaa R (2007) Drainage of forests in Finland. Irrig Drain 56(1):151–159
Pirinen P, Simola H, Aalto J, Kaukoranta J, Karlsson P, Ruuhela R (2012) Tilastoja Suomen ilmastosta 19812010 (Climatological statistics of Finland 1981–2010)
Prévost M, Plamondon AP, Belleau P (1999) Effects of drainage of a forested peatland on water quality and quantity. J Hydrol 214(1):130–143
Ronkanen AK, Kløve B (2005) Hydraulic soil properties of peatlands treating municipal wastewater and peat harvesting runoff. Mires and Peat 56(2):43–46
Sen D, Garg N (2002) Efficient algorithm for gradually varied flows in channel networks. J Irrig Drain Eng 128(6):351–357
Smolander M (2011) Vesitase ojitetussa suometsikössä (abstract: Water balance in a drained peatland forest). Master's Thesis, Aalto University, School of engineering, Department of Civil and Environmental Engineering
Stenberg L, Finér L, Nieminen M, Sarkkola S, Koivusalo H (2014) Quantification of ditch bank erosion in a drained forested catchment. Boreal Environ Res 20 (in press)
Strelkoff TS, Falvey HT (1993) Numerical methods used to model unsteady canal flow. J Irrig Drain Eng 119(4): 637–655
Szymkiewicz R (2010) Numerical modeling in open channel hydraulics. Springer, Dordrecht
Turunen M (2011) Pellon vesitaseen ja salaojitusmenetelmien toimivuuden analyysi (abstract: Analysis of the water balance and subsurface drainage methods in an agricultural field). Master's Thesis, Aalto University, School of engineering, Department of Civil and Environmental Engineering
Tuukkanen T, Koivusalo H, Marttila H, Leinonen A, Kløve B, Laurén A, Finér L (2012) A GIS-based model for ditch erosion risk assessment in peatland forestry. In: Collins A, Golosov V, Horowitz A, Lu X, Stone M, Walling D, Zhang X (eds) Erosion and Sediment Yields in the Changing Environment, International Association of Hydrological Sciences, pp 221–227

van Genuchten M (1980) A closed-form equation for predicting the hydraulic conductivity of unsaturated soils. Soil Sci Soc Am J 44(5):892–898

von Post L (1922) Sveriges geologiska undersoknings torvinventering och nogra av dess hittils vunna resultat [SGU peat inventory and some preliminary results]. Svenska Mosskulturforeningens Tidskrift 36:1–37

Wigmosta MS, Vail LW, Lettenmaier DP (1994) A distributed hydrology-vegetation model for complex terrain. Water Resour Res 30(6):1665–1679

Yen B (2002) Open channel flow resistance. J Hydraul Eng 128(1):20–39

Zhu D, Chen Y, Wang Z, Liu Z (2011) Simple, robust, and efficient algorithm for gradually varied subcritical flow simulation in general channel networks. J Hydraul Eng 137(7):766–774